Recovering hidden signals of statistical anisotropy from a masked or partial CMB sky

Pavan K. Aluri
Nidhi Pant
Aditya Rotti
Tarun Souradeep

Based on **arXiv:1506.00550**

Isotropy violation : Eg. Dipole anisotropy

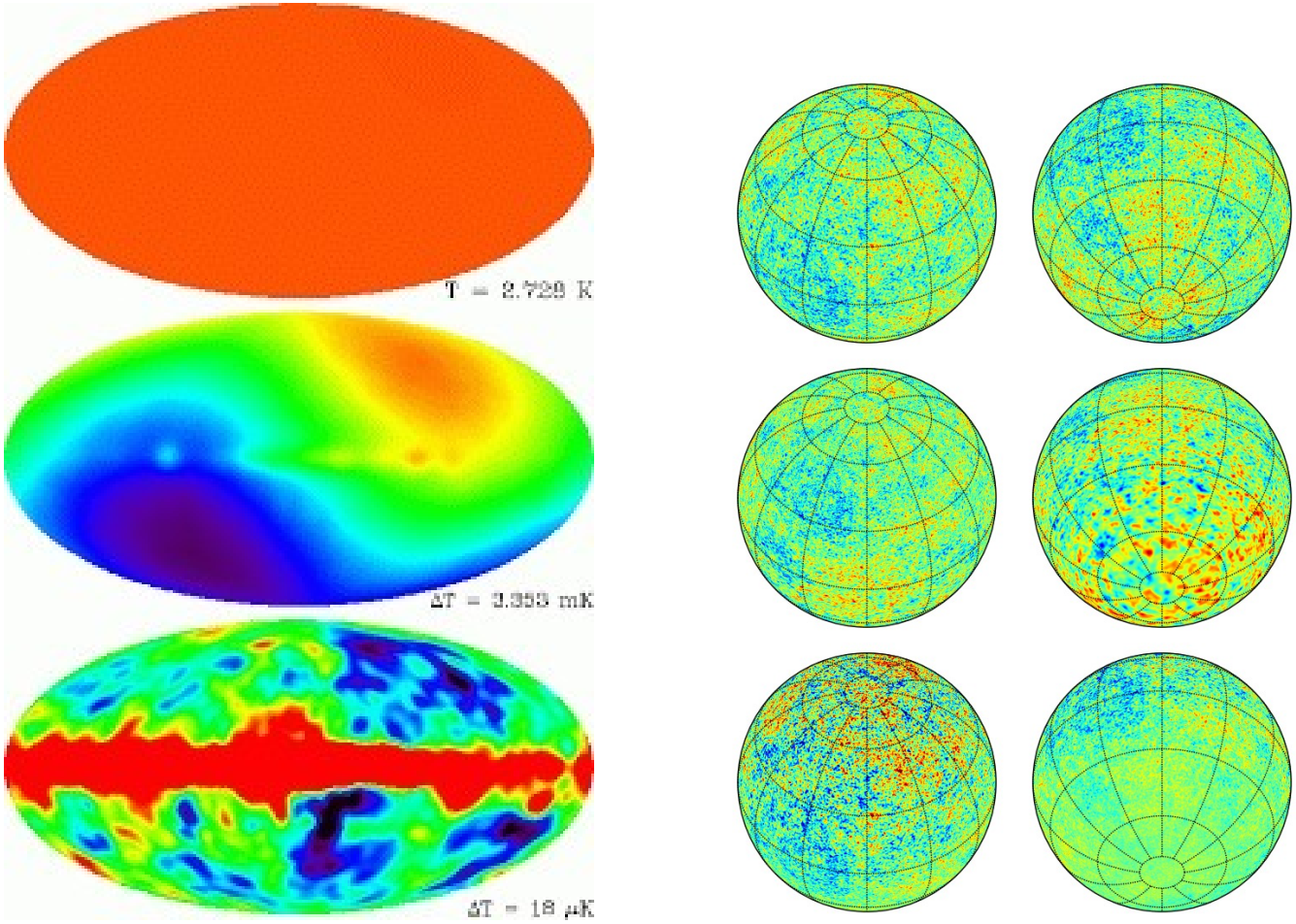

Figure: **Left:** CMB anisotropies as observed by NASA's COBE satellite, in Mollweide projection. **Right:** High$-l$ effects of exaggerated Doppler boost on CMB (PLANCK2013-XXVII).

Isotropy violation : Eg. Doppler Boost

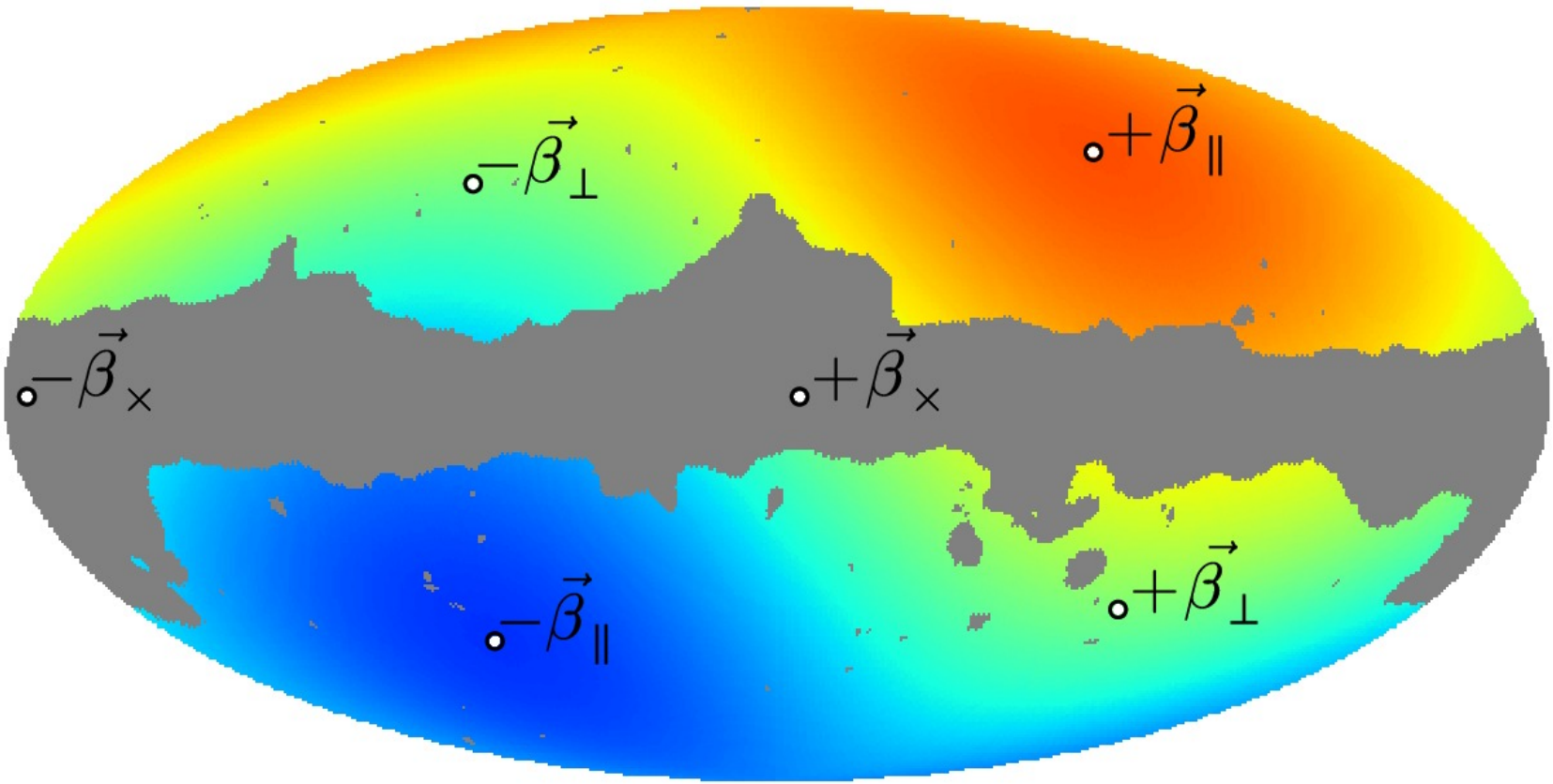

Figure: Doppler boost signal recovered in PLANCK2013-XXVII, using high$-l$ correlation from the multipole range $l = [500, 2000]$.

Isotropy violation : Eg. Low−/ modulation

Dipole modulation of CMB temperature anisotropies :

$$\Delta T(\hat{n}) = \Delta T_{iso}(\hat{n})(1 + A\,\hat{\lambda}\cdot\hat{n})\,.$$

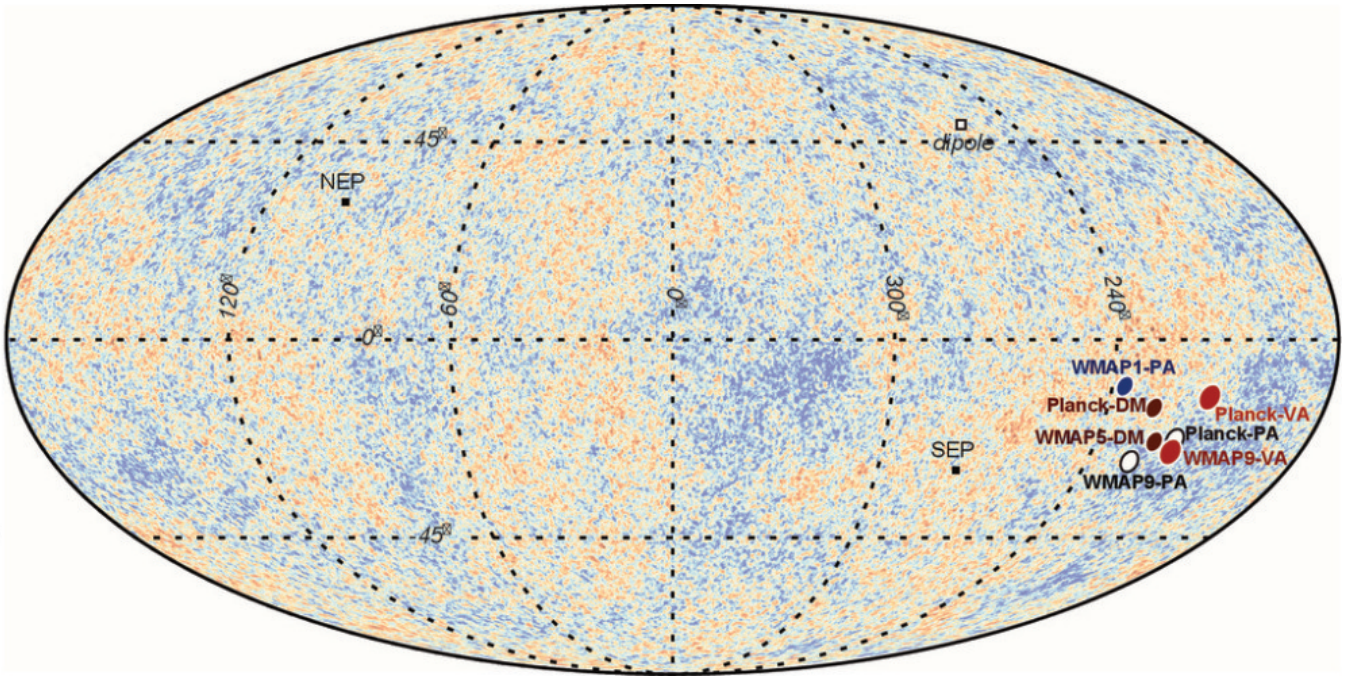

Figure: Y. Akrami et al., 2014, ApJ, 784, L42

CMB Foreground : spatial extent

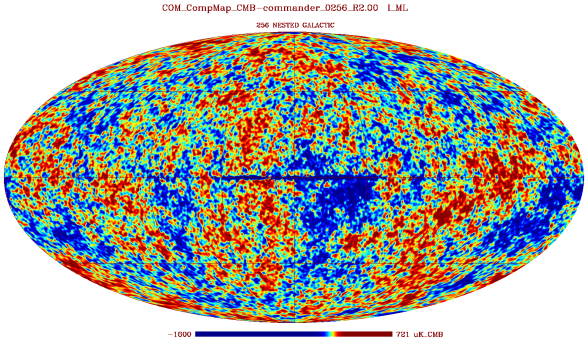

(a) CMB

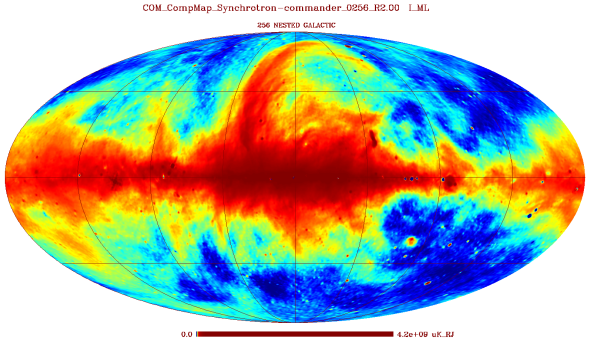

(b) Synchrotron

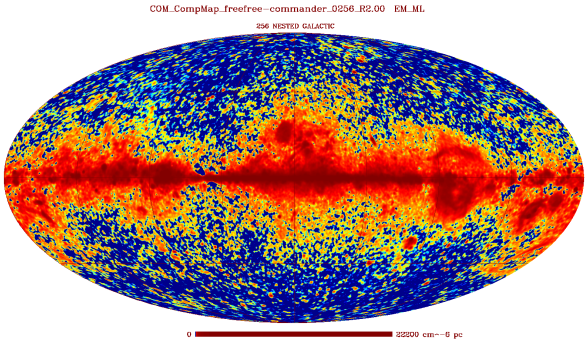

(c) Free-Free

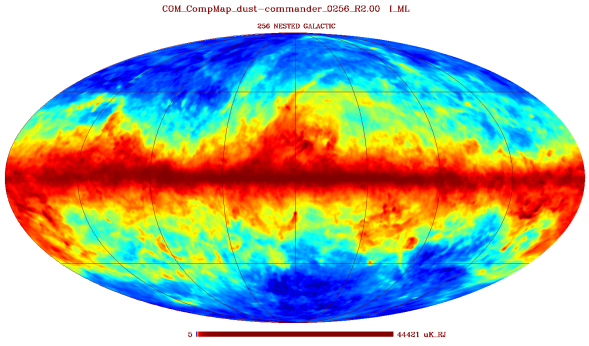

(d) Thermal Dust

Figure: `Commander` estimated CMB and three foreground components from PLANCK 2015 data release.

CMB Foreground : frequency dependence

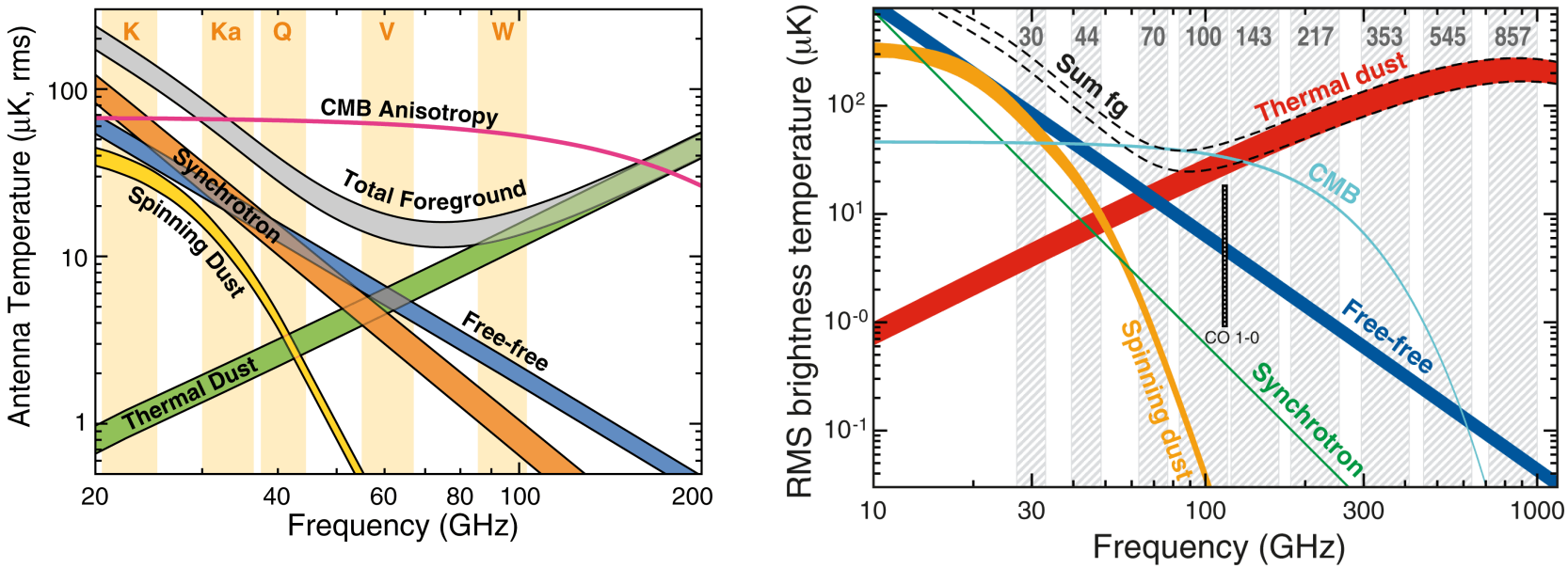

Figure: Variation of some of the foreground component levels in the frequency range in which WMAP and PLANCK made their observations.

Foreground mask : common/freq. specific

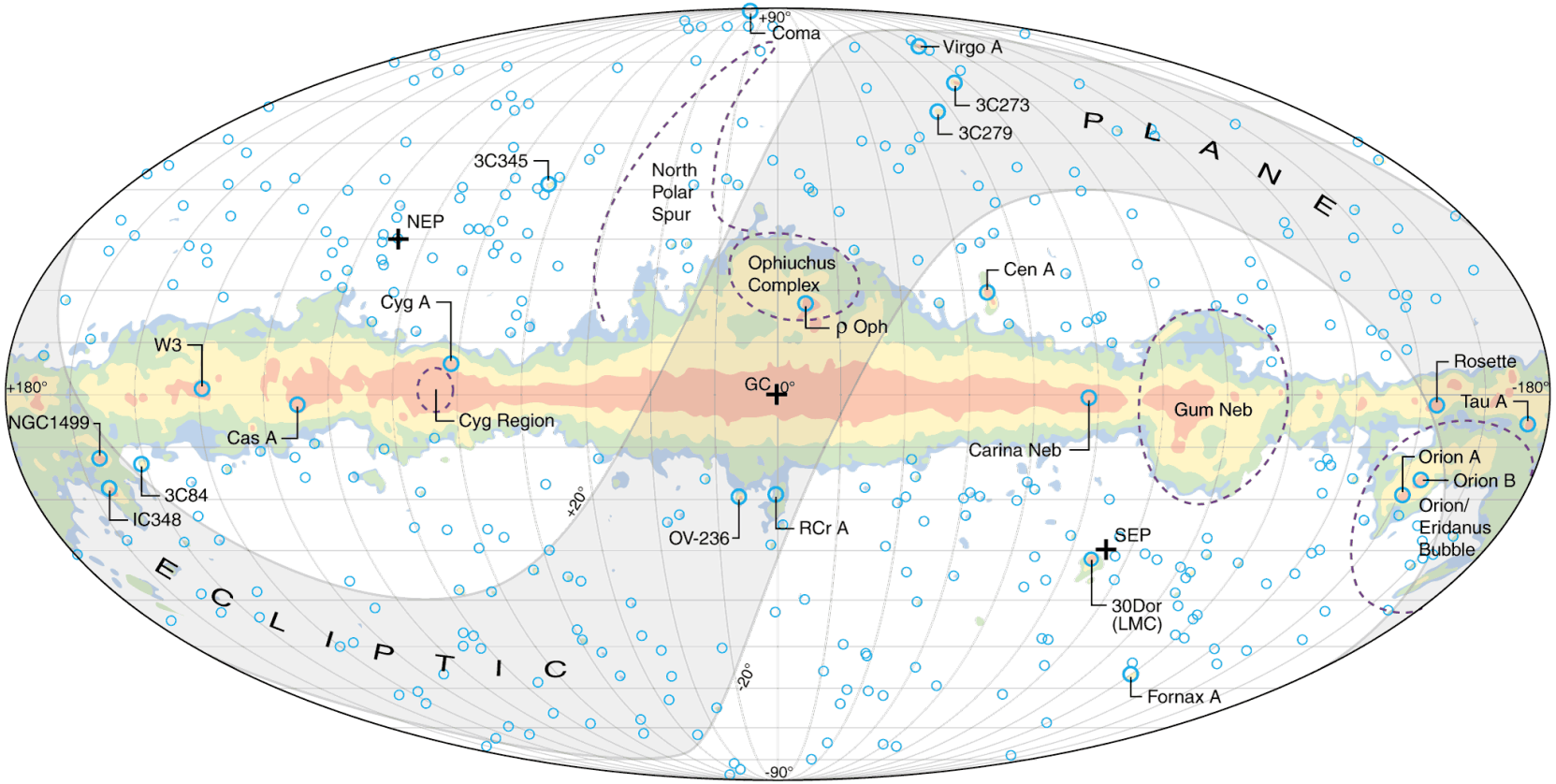

Figure: Contours of foreground level in WMAP data. Masking is necessary to prevent leakage of/bias due to foreground contamination in estimating quantities of interest.

BipoSH

$$T(\theta,\phi) = \sum_{l=0}^{\infty} \sum_{m=-l}^{l} a_{lm}\, Y_{lm}(\theta,\phi)\,. \tag{1}$$

Two-point correlation function :

$$C(\hat{n},\hat{n}') = \langle \Delta T(\hat{n})\, \Delta T(\hat{n}') \rangle\,. \tag{2}$$

If CMB is isotropic then $C(\hat{n},\hat{n}') \to C(\Theta = \hat{n}\cdot\hat{n}')$, otherwise

$$C(\hat{n}_1,\hat{n}_2) = \langle \Delta T(\hat{n}_1) \Delta T(\hat{n}_2) \rangle \tag{3}$$

$$A^{LM}_{l_1 l_2} = \int d\Omega_1 d\Omega_2\, C(\hat{n}_1,\hat{n}_2) \{ Y_{l_1}(\hat{n}_1) \otimes Y_{l_2}(\hat{n}_2) \}^*_{LM} \tag{4}$$

Bipolar Spherical Harmonic (BipoSH) coefficients :

$$A^{LM}_{l_1 l_2} = \sum_{m_1 m_2} a_{l_1 m_1}\, a_{l_2 m_2}\, C^{LM}_{l_1 m_1 l_2 m_2}\,. \tag{5}$$

Effect of velocity boost on CMB

Doppler boost = dipole + aberration × freq. dep. modulation

$$\Delta T(\hat{n}) = T_0 \vec{\beta} \cdot \hat{n} + \Delta T' \left(\hat{n} - \nabla(\vec{\beta} \cdot \hat{n}) \right) \left(1 + b_\nu \vec{\beta} \cdot \hat{n} \right), \quad (6)$$

where

$\vec{\beta} = \vec{v}/c$,
ΔT = boosted temperature anisotropies,
$\Delta T'$ = unboosted temperature anisotropies,
$b_\nu = \frac{\nu}{\nu_0} \coth\left(\frac{\nu}{2\nu_0}\right) - 1$ and,
$\nu_0 = k_B T_{cmb}/h$.

The BipoSH coefficients of Doppler boosted CMB anisotropies upto $\mathcal{O}(\beta)$ are given by

$$A^{LM}_{l_1 l_1} = \left(A^{LM}_{l_1 l_2}\right)^{iso.\ cmb} + \beta_{LM} H^L_{l_1 l_2} . \quad (7)$$

BipoSH Doppler recovery : Fullsky

Here $H^L_{l_1 l_2}$ is a function describing Doppler boost effects in BipoSH space.

For $L > 0$, one can define a *minimum variance estimator* as

$$\beta_{LM} = \sum_{l_1 l_2} w^L_{l_1 l_2} \frac{A^{LM}_{l_1 l_2}}{H^L_{l_1 l_1}} \,, \tag{8}$$

with weights (that add upto 'one') and reconstruction noise given by

$$w^L_{l_1 l_2} = \frac{(H^L_{l_1 l_2})^2}{C_{l_1} C_{l_2}} \left[\sum_{l_1 l_2} \frac{(H^L_{l_1 l_2})^2}{C_{l_1} C_{l_2}} \right]^{-1} , \tag{9}$$

$$N_L = \left[\sum_{l_1 l_2} \frac{(H^L_{l_1 l_2})^2}{2\, C_{l_1} C_{l_2}} \right]^{-1} , \tag{10}$$

BipoSH Doppler rec. : Fullsky : Results

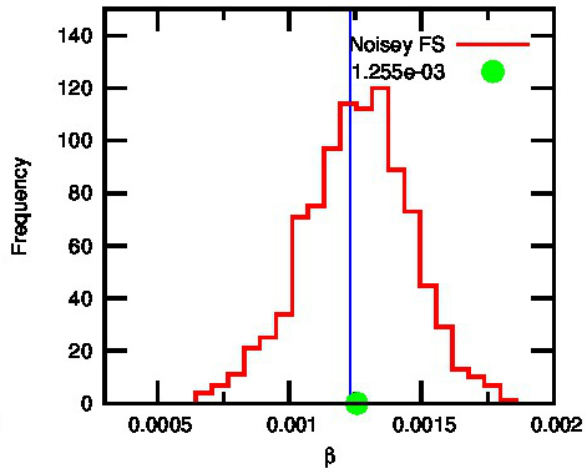

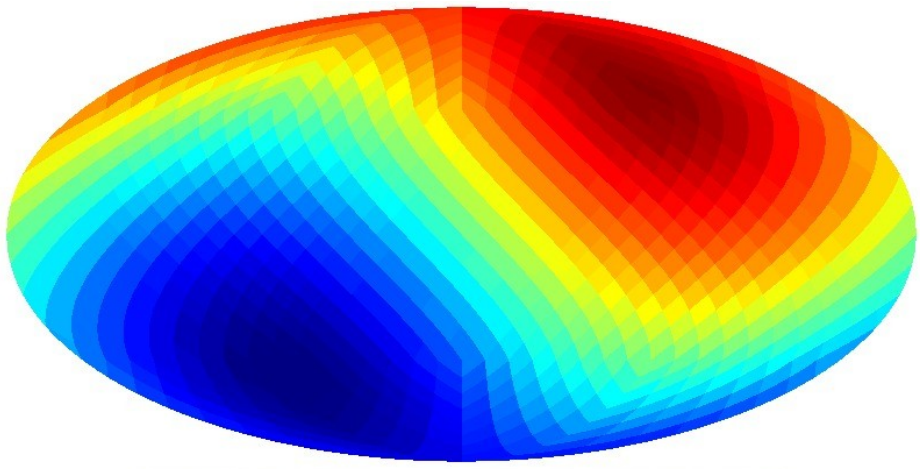

Figure: Doppler signal recovery from full sky estimator from simulated full sky Doppler boosted CMB maps generated using `CoNIGS` [S. Mukherjee S.& T. Souradeep (2014)] with nominal PLANCK noise level for 217 GHz.

BipoSH Doppler recovery - Masked sky

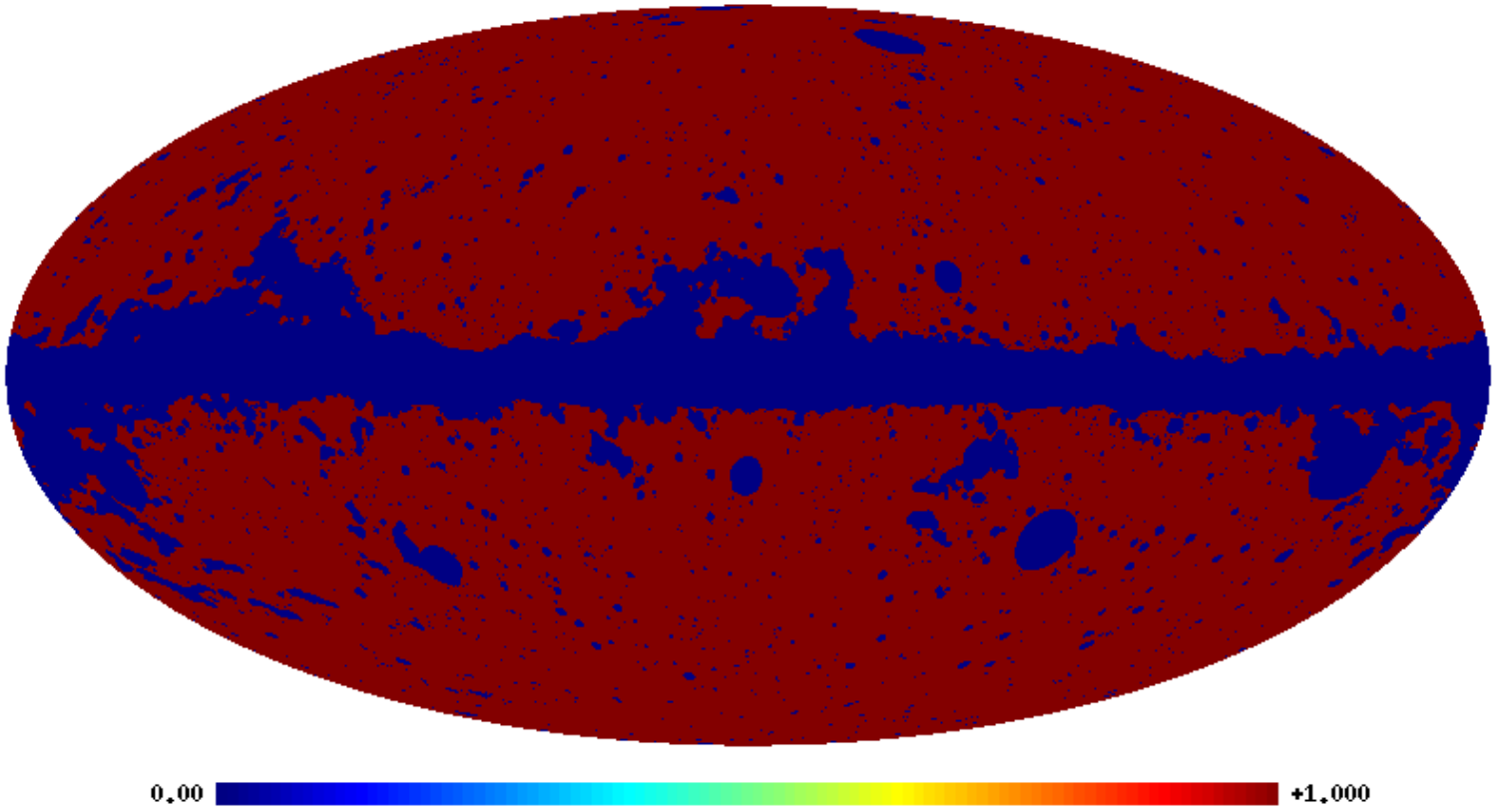

Figure: Common analysis mask to exclude regions with significant foreground contamination used in Planck 2015 data.

BipoSH Doppler rec. - Masked sky (contd.)

Masked sky BipoSH's in terms of full sky BipoSH :

$$\tilde{A}^{LM}_{l_1 l_2} = \sum_{l_3 l_4} \frac{\Pi_{l_3}\Pi_{l_4}}{\sqrt{4\pi}} \sum_{l_5 l_6} \frac{\Pi_{l_5}\Pi_{l_6}}{\sqrt{4\pi}} C^{l_1 0}_{l_3 0 l_5 0} C^{l_2 0}_{l_4 0 l_6 0} \times \sum_{L' M' J K} \begin{Bmatrix} L & l_1 & l_2 \\ L' & l_3 & l_4 \\ J & l_5 & l_6 \end{Bmatrix} \times \Pi_{L'}\Pi_J A^{L' M'}_{l_3 l_4} W^{JK}_{l_5 l_6} C^{LM}_{L' M' JK} \,, \quad (11)$$

This is a generalization of the pseudo$-C_l$ MASTER algorithm of *Hivon et al. (2002)* relating masked and full sky C_l :

$$\tilde{C}_l = \sum_{ll'} M_{ll'} C_{l'} \quad (12)$$

since $A^{00}_{ll'} \propto C_l \delta_{ll'}$.

BipoSH Doppler rec. - Masked sky (contd.)

BipoSH due to Doppler boosted CMB anisotropies from a masked sky :

$$\tilde{A}^{LM}_{l_1 l_2} = \left(\tilde{A}^{LM}_{l_1 l_2}\right)^{iso.cmb} + \sum_{L'M'} \beta_{L'M'} K^{L'M'}_{LMl_1 l_2} \,. \tag{13}$$

Further simplifications :

- The modified shape function (MSF), $K^{L'M'}_{LMll'}$, is diagonal i.e., $M = M'$
- There is no significant leakage from intrinsic Doppler signal $L' = 1$ to $L \neq 1$

Under these approximations : $L = L'$ (=1) and $M = M'$ we have

$$\tilde{A}^{LM}_{l_1 l_2} = \left(\tilde{A}^{LM}_{l_1 l_2}\right)^{iso.cmb} + \beta_{LM} K^{LM}_{LMl_1 l_2} \,. \tag{14}$$

BipoSH Doppler rec. - Masked sky (contd.)

With these approximations we can define an estimator for masked sky as

$$\hat{\beta}_{LM} = \sum_{l_1 l_2} \hat{w}^{L}_{l_1 l_2} \frac{\hat{\mathcal{A}}^{LM}_{l_1 l_2}}{K^{LM}_{L\,M\,l_1\,l_2}} \,, \tag{15}$$

where

$$\hat{w}^{L}_{l_1 l_2} = \frac{1}{\sum_M \frac{\hat{\sigma}^{LM}_{l_1 l_2}}{(K^{LM}_{LMl_1 l_2})^2}} \left[\sum_{l_1 l_2} \frac{1}{\sum_M \frac{\hat{\sigma}^{LM}_{l_1 l_2}}{(K^{LM}_{LMl_1 l_2})^2}} \right]^{-1} , \tag{16}$$

$$\hat{\mathcal{A}}^{LM}_{l_1 l_2} = \tilde{A}^{LM}_{l_1 l_2} - \langle \tilde{A}^{LM}_{l_1 l_2} \rangle_{iso.cmb} \,, \tag{17}$$

$$\hat{\sigma}^{LM}_{l_1 l_2} = \langle |\tilde{A}^{LM}_{l_1 l_2}|^2 \rangle_{iso.cmb} - |\langle \tilde{A}^{LM}_{l_1 l_2} \rangle_{iso.cmb}|^2 \,. \tag{18}$$

- One more simplification : BipoSH covariance is diagonal

$$\langle \mathcal{A}^{LM}_{l_1,l_2} \mathcal{A}^{LM*}_{l'_1,l'_2} \rangle \rightarrow \left(\hat{\sigma}^{LM}_{l_1 l_2} \right)^2 \delta_{l_1 l'_1} \delta_{l_2 l'_2}$$

BipoSH Doppler rec. - Masked sky (contd.)

Justification - 1 :

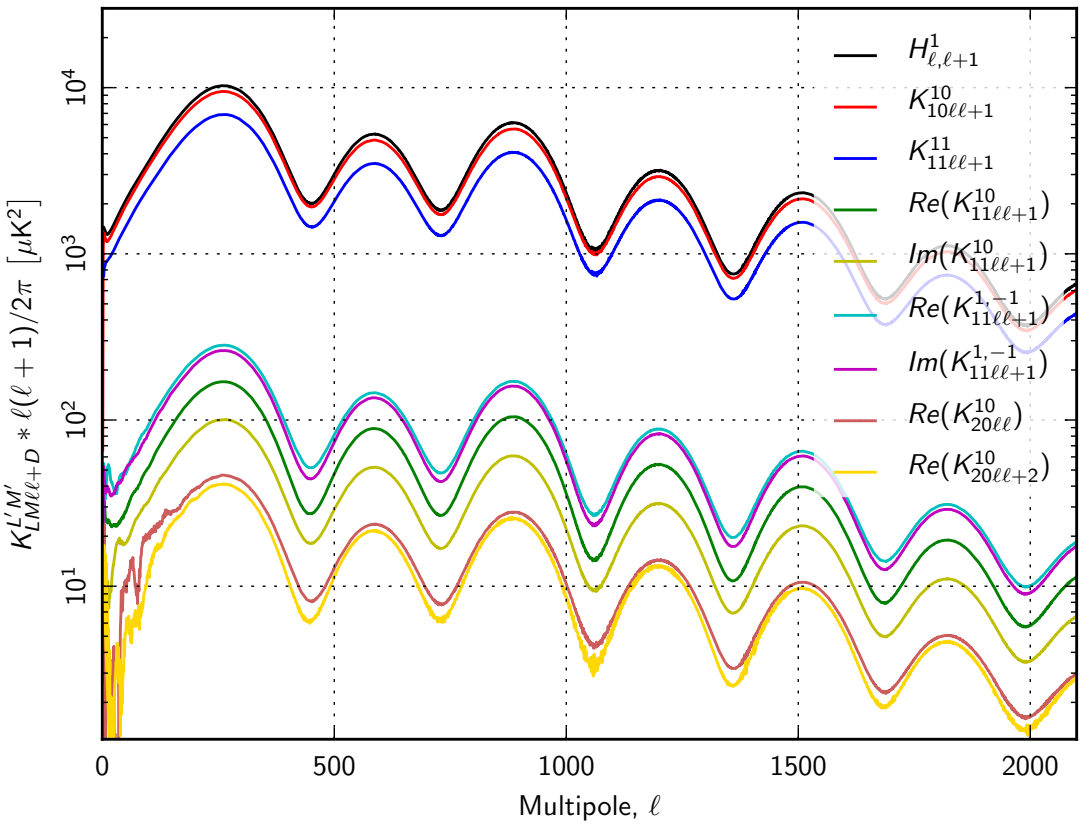

Figure: MSF of the apodized common analysis mask used in Planck 2015 data.

BipoSH Doppler rec. - Masked sky (contd.)

Justification - 2 :

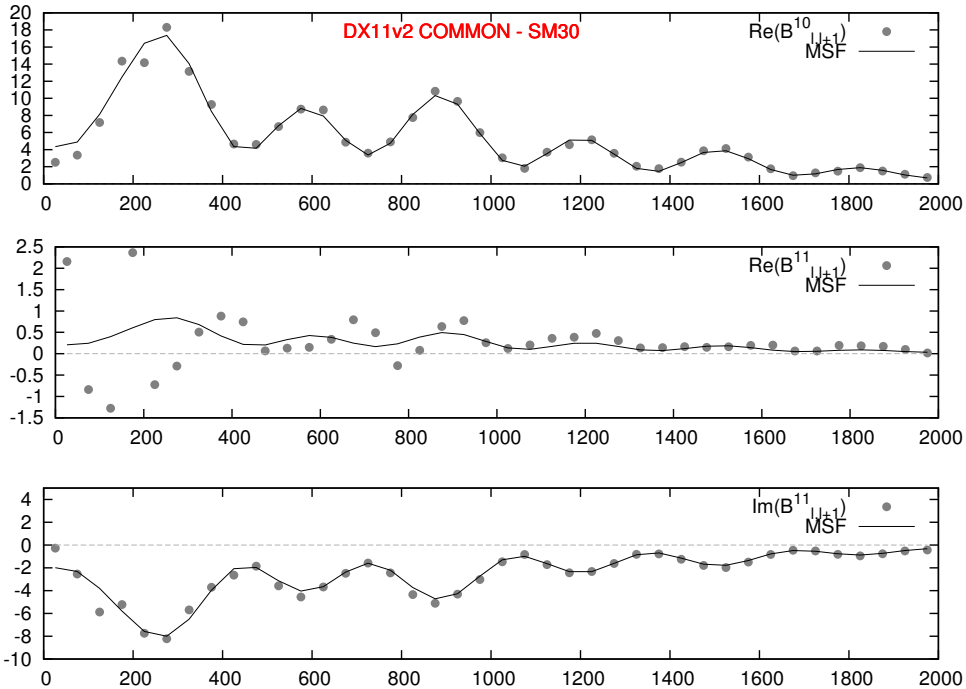

Figure: Validating the consistency of the relation $\tilde{A}^{LM}_{l_1 l_2} - \left(\tilde{A}^{LM}_{l_1 l_2}\right)^{iso.cmb} = \beta_{LM} K^{LM}_{LMl_1 l_2}$, between MSF in diagonal approximation and mask bias corrected anisotropic BipoSH coefficients.

BipoSH Doppler rec. - Masked sky (contd.)

Justification - 3 :

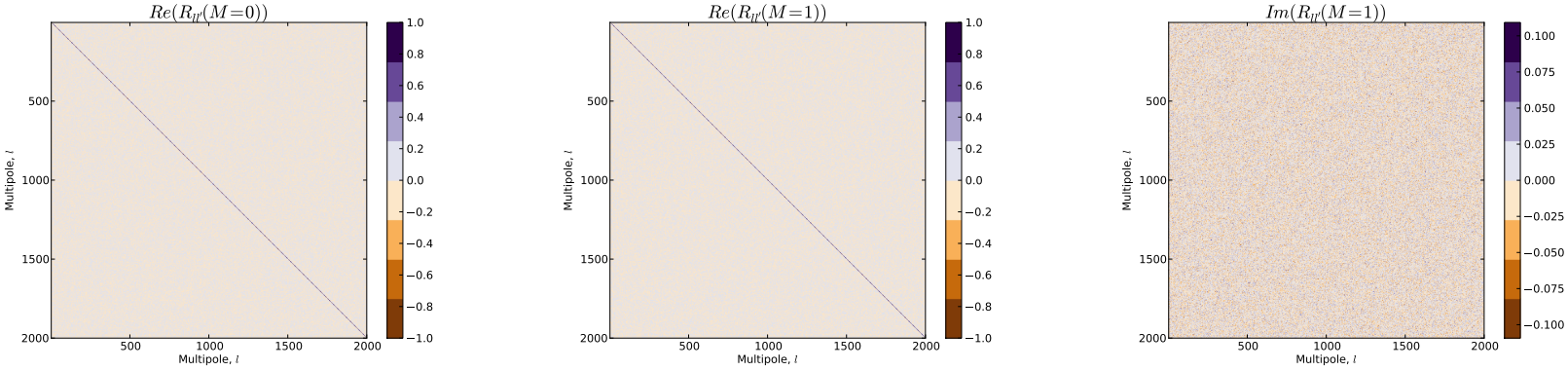

Figure: Validating the diagonal approximation to the covariance of bias corrected BipoSH coefficients : $\langle \mathcal{A}^{LM}_{l_1,l_2} \mathcal{A}^{LM*}_{l'_1,l'_2} \rangle \rightarrow \left(\hat{\sigma}^{LM}_{l_1 l_2}\right)^2 \delta_{l_1 l'_1} \delta_{l_2 l'_2}$.

Normalized BipoSH covariance matrix is defined as,

$$R_{ll'} = \frac{C_{ll'}}{\sqrt{|C_{ll}||C_{l'l'}|}} \tag{19}$$

$$C_{ll'} = \langle A^{1M}_{ll+1} A^{1M*}_{l'l'+1} \rangle \tag{20}$$

Paper describing the methodology

A novel approach to reconstructing signals of isotropy violation from a masked CMB sky

Pavan K. Aluri,[1] Nidhi Pant,[1] Aditya Rotti,[1,2] and Tarun Souradeep[1]

[1]*IUCAA, Pune - 411007, India*
[2]*Florida State University, Tallahassee, FL 32304, USA*

Statistical isotropy (SI) is one of the fundamental assumptions made in cosmological model building. This assumption is now being rigorously tested using the almost full sky measurements of the CMB anisotropies. A major hurdle in any such analysis is to handle the large biases induced due to the process of masking. We have developed a new method of analysis, using the bipolar spherical harmonic basis functions, in which we semi-analytically evaluate the modifications to SI violation induced by the mask. The method developed here is generic and can be potentially used to search for any arbitrary form of SI violation. We specifically demonstrate the working of this method by recovering the Doppler boost signal from a set of simulated, masked CMB skies.

PACS numbers: 98.70.Vc, 98.80.Es

Figure: arXiv:1506.00550

Results

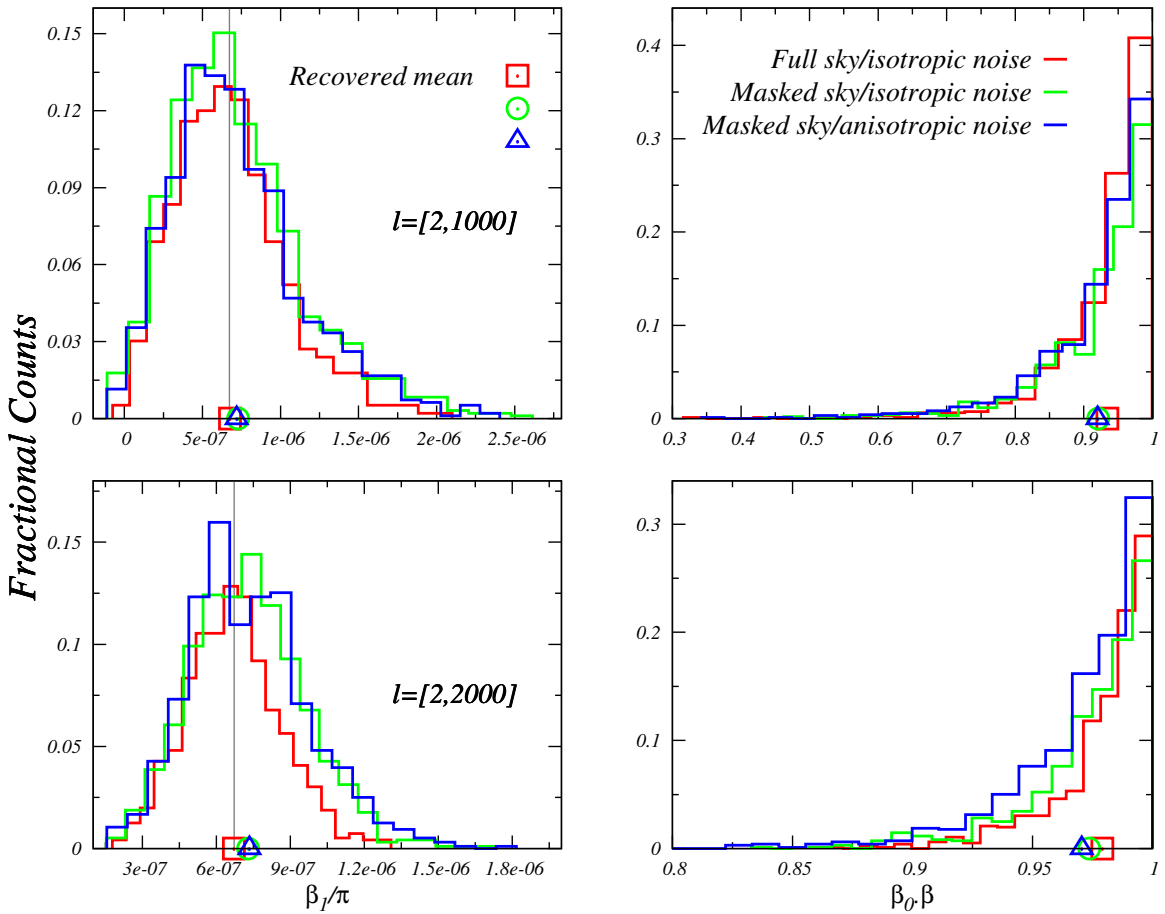

Figure: Doppler signal estimated from masked simulated Doppler boosted CMB skies, from different mutlipole bin windows.

Application to data : PLANCK 2015 I&S

***Planck* 2015 results. XVI. Isotropy and statistics of the CMB**

Planck Collaboration: P. A. R. Ade[89], N. Aghanim[60], Y. Akrami[65,103], P. K. Aluri[55], M. Arnaud[75], M. Ashdown[72,6], J. Aumont[60], C. Baccigalupi[88], A. J. Banday[100,9,*], R. B. Barreiro[67], N. Bartolo[32,68], S. Basak[88], E. Battaner[101,102], K. Benabed[61,99], A. Benoît[58], A. Benoit-Lévy[26,61,99], J.-P. Bernard[100,9], M. Bersanelli[35,49], P. Bielewicz[85,9,88], J. J. Bock[69,11], A. Bonaldi[70], L. Bonavera[67], J. R. Bond[8], J. Borrill[14,94], F. R. Bouchet[61,92], F. Boulanger[60], M. Bucher[1], C. Burigana[48,33,50], R. C. Butler[48], E. Calabrese[97], J.-F. Cardoso[76,1,61], B. Casaponsa[67], A. Catalano[77,74], A. Challinor[64,72,12], A. Chamballu[75,16,60], H. C. Chiang[29,7], P. R. Christensen[86,38], S. Church[96], D. L. Clements[56], S. Colombi[61,99], L. P. L. Colombo[25,69], C. Combet[77], D. Contreras[24], F. Couchot[73], A. Coulais[74], B. P. Crill[69,11], M. Cruz[21], A. Curto[67,6,72], F. Cuttaia[48], L. Danese[88], R. D. Davies[70], R. J. Davis[70], P. de Bernardis[34], A. de Rosa[48], G. de Zotti[45,88], J. Delabrouille[1], F.-X. Désert[54], J. M. Diego[67], H. Dole[60,59], S. Donzelli[49], O. Doré[69,11], M. Douspis[60], A. Ducout[61,56], X. Dupac[39], G. Efstathiou[64], F. Elsner[26,61,99], T. A. Enßlin[82], H. K. Eriksen[65], Y. Fantaye[37], J. Fergusson[12], R. Fernandez-Cobos[67], F. Finelli[48,50], O. Forni[100,9], M. Frailis[47], A. A. Fraisse[29], E. Franceschi[48], A. Frejsel[86], A. Frolov[91], S. Galeotta[47], S. Galli[71], K. Ganga[1], C. Gauthier[1,81], T. Ghosh[60], M. Giard[100,9], Y. Giraud-Héraud[1], E. Gjerløw[65], J. González-Nuevo[20,67], K. M. Górski[69,104], S. Gratton[72,64], A. Gregorio[36,47,53], A. Gruppuso[48], J. E. Gudmundsson[29], F. K. Hansen[65], D. Hanson[83,69,8], D. L. Harrison[64,72], S. Henrot-Versillé[73], C. Hernández-Monteagudo[13,82], D. Herranz[67], S. R. Hildebrandt[69,11], E. Hivon[61,99], M. Hobson[6], W. A. Holmes[69], A. Hornstrup[17], W. Hovest[82], Z. Huang[8], K. M. Huffenberger[27], G. Hurier[60], A. H. Jaffe[56], T. R. Jaffe[100,9], W. C. Jones[29], M. Juvela[28], E. Keihänen[28], R. Keskitalo[14], J. Kim[82], T. S. Kisner[79], J. Knoche[82], M. Kunz[18,60,3], H. Kurki-Suonio[28,44], G. Lagache[5,60], A. Lähteenmäki[2,44], J.-M. Lamarre[74], A. Lasenby[6,72], M. Lattanzi[33], C. R. Lawrence[69], R. Leonardi[39], J. Lesgourgues[62,98], F. Levrier[74], M. Liguori[32,68], P. B. Lilje[65], M. Linden-Vørnle[17], H. Liu[86,38], M. López-Caniego[39,67], P. M. Lubin[30], J. F. Macías-Pérez[77], G. Maggio[47], D. Maino[35,49], N. Mandolesi[48,33], A. Mangilli[60,73], D. Marinucci[37], M. Maris[47], P. G. Martin[8], E. Martínez-González[67], S. Masi[34], S. Matarrese[32,68,42], P. McGehee[57], P. R. Meinhold[30], A. Melchiorri[34,51], L. Mendes[39], A. Mennella[35,49], M. Migliaccio[64,72], K. Mikkelsen[65], S. Mitra[55,69], M.-A. Miville-Deschênes[60,8], D. Molinari[67,48], A. Moneti[61], L. Montier[100,9], G. Morgante[48], D. Mortlock[56], A. Moss[96], D. Munshi[89], J. A. Murphy[84], P. Naselsky[86,38], F. Nati[29], P. Natoli[33,4,48], C. B. Netterfield[22], H. U. Nørgaard-Nielsen[17], F. Noviello[70], D. Novikov[80], I. Novikov[86,80], C. A. Oxborrow[17], F. Paci[88], L. Pagano[34,51], F. Pajot[60], N. Pant[55], D. Paoletti[48,50], F. Pasian[47], G. Patanchon[1], T. J. Pearson[11,57], O. Perdereau[73], L. Perotto[77], F. Perrotta[88], V. Pettorino[43], F. Piacentini[34], M. Piat[1], E. Pierpaoli[25], D. Pietrobon[69], S. Plaszczynski[73], E. Pointecouteau[100,9], G. Polenta[4,46], L. Popa[63], G. W. Pratt[75], G. Prézeau[11,69], S. Prunet[61,99], J.-L. Puget[60], J. P. Rachen[23,82], R. Rebolo[66,15,19], M. Reinecke[82], M. Remazeilles[70,60,1], C. Renault[77], A. Renzi[37,52], I. Ristorcelli[100,9], G. Rocha[69,11], C. Rosset[1], M. Rossetti[35,49], A. Rotti[55], G. Roudier[1,74,69], J. A. Rubiño-Martín[66,19], B. Rusholme[57], M. Sandri[48], D. Santos[77], M. Savelainen[28,44], G. Savini[87], D. Scott[24], M. D. Seiffert[69,11], E. P. S. Shellard[12], T. Souradeep[55], L. D. Spencer[89], V. Stolyarov[6,72,95], R. Stompor[1], R. Sudiwala[89], R. Sunyaev[82,93], D. Sutton[64,72], A.-S. Suur-Uski[28,44], J.-F. Sygnet[61], J. A. Tauber[40], L. Terenzi[41,48], L. Toffolatti[20,67,48], M. Tomasi[35,49], M. Tristram[73], T. Trombetti[48], M. Tucci[18], J. Tuovinen[10], L. Valenziano[48], J. Valiviita[28,44], B. Van Tent[78], P. Vielva[67], F. Villa[48], L. A. Wade[69], B. D. Wandelt[61,99,31], I. K. Wehus[69], D. Yvon[16], A. Zacchei[47], J. P. Zibin[24], and A. Zonca[30]

Figure: Planck 2015 results. XVI. Isotropy and statistics of the CMB - arXiv:1506.07135

Application to PLANCK 2015 data (contd.)

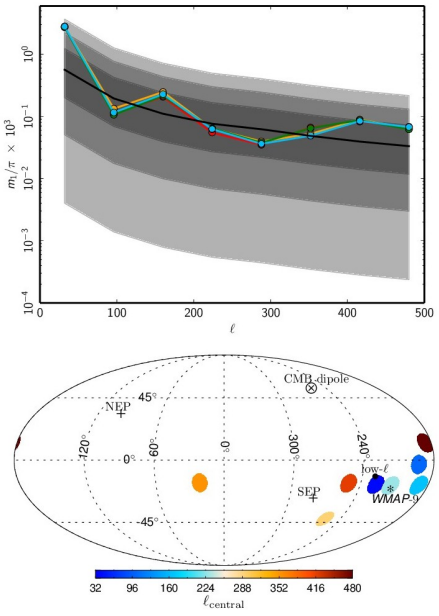

Fig. 32. *Top:* Measured dipole modulation ($L = 1$) power in non-overlapping CMB multipole bins for `Commander` (red), `NILC` (orange), `SEVEM` (green), and `SMICA` (blue) as determined from a BipoSH analysis of the data. The power in the dipole of the modulation field is a χ^2-distributed variable with 3 degrees of freedom. The shaded regions in the plot depict, in dark-grey, grey, and light-grey respectively, the 1, 2, and 3σ equivalent intervals of the distribution function derived from simulations, while the solid black line denotes its median. Significant power in the dipole modulation is seen to be limited to $\ell = 2$–64 and does not extend to higher multipoles. *Bottom:* Dipole modulation direction as determined from the `SMICA` map. The directions found from the other component separation maps are consistent with this analysis. The coloured circles denote the central value of the multipole bin used in the analysis, as specified in the colour bar. The low-ℓ and WMAP-9 directions are identical to those in Fig. 35.

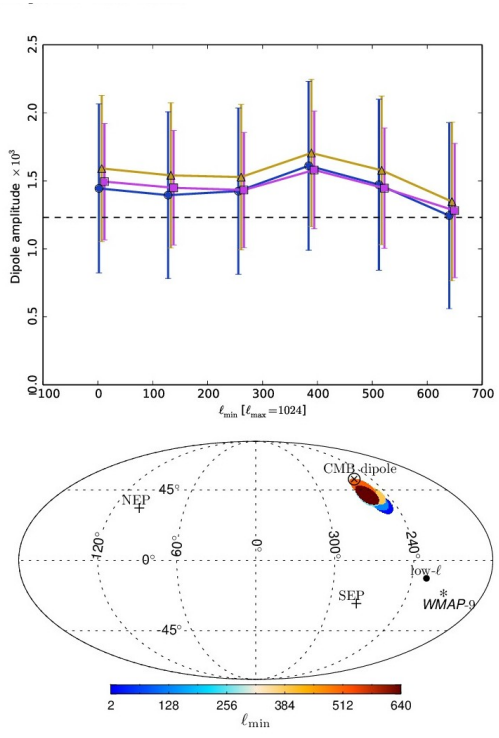

Fig. 34. *Top:* Amplitude $|\beta|$ of the Doppler boost from the `SEVEM-100`, `SEVEM-143`, and `SEVEM-217` maps for different multipole bins determined using a BipoSH analysis. The maximum multipole of each bin is fixed at $\ell_{\rm max} = 1024$, while $\ell_{\rm min}$ is incremented from $\ell = 2$ to $\ell = 640$ in steps of $\Delta\ell = 128$. The dashed line corresponds to the actual dipole boost amplitude, $|\boldsymbol{\beta}| = 1.23 \times 10^{-3}$. *Bottom:* Doppler boost direction $\hat{\beta}$ measured in Galactic coordinates from `SEVEM-217`. The coloured circles denote $\ell_{\rm min}$ used in the analysis, while $\ell_{\rm max} = 1024$ is held fixed. The low-ℓ and WMAP-9 directions are identical to those in Fig. 35.

(a) Low−l dipole modulation

(b) Doppler boost

Application to PLANCK 2015 data (contd.)

Table 24. Amplitude (A) and direction of the dipole modulation in Galactic coordinates as estimated for the multipole range $\ell \in [2, 64]$ using a BipoSH analysis. The measured values of the dipole amplitude and direction are consistent for all maps.

Method	A	Direction (l, b) [°]
`Commander` . .	0.067 ± 0.023	$(230, -18) \pm 31$
`NILC`	0.069 ± 0.022	$(228, -17) \pm 30$
`SEVEM`	0.067 ± 0.023	$(230, -17) \pm 31$
`SMICA`	0.069 ± 0.022	$(228, -18) \pm 30$

(c) Low−l dipole modulation

Table 25. The Doppler boost amplitude ($|\boldsymbol{\beta}|$) and direction in Galactic coordinates derived over the multipole range $\ell \in [640, 1024]$ as evaluated from a BipoSH analysis. The errors are estimated from an identical analysis of a set of 1000 Doppler boosted simulations for each frequency.

Map	$\lvert\boldsymbol{\beta}\rvert \times 10^{-3}$	Direction (l, b) [°]
`SEVEM-100`	1.24 ± 0.66	$(277, 40) \pm 50$
`SEVEM-143`	1.35 ± 0.56	$(264, 39) \pm 39$
`SEVEM-217`	1.28 ± 0.45	$(257, 42) \pm 32$

(d) Doppler boost

Acknowledgements

- We acknowledge the use of NASA's WMAP satellite data made available at LAMBDA site, and ESA's PLANCK satellite data available at PLA web page.
- We acknowledge the use of `HEALPix` package created for representing/manipulating data on a sphere for CMB analysis.
- Some of the images are taken from NASA's WMAP, and ESA's PLANCK mission pages.

Thank You

for your patience